JCB Article

Regulated splicing of the fibronectin EDA exon is essential for proper skin wound healing and normal lifespan

Andrés F. Muro,[1] Anil K. Chauhan,[1] Srecko Gajovic,[2] Alessandra Iaconcig,[1] Fabiola Porro,[1] Giorgio Stanta,[1,3] and Francisco E. Baralle[1]

[1]International Centre for Genetic Engineering and Biotechnology, 34012 Trieste, Italy
[2]Croatian Institute for Brain Research, School of Medicine, University of Zagreb, 10000 Zagreb, Croatia
[3]Department of Clinical, Morphological and Technological Sciences, University of Trieste, 34100 Trieste, Italy

Fibronectins (FNs) are multifunctional high molecular weight glycoproteins present in the blood plasma and in the ECMs of tissues. The FN primary transcript undergoes alternative splicing in three regions generating up to 20 main different variants in humans. However, the precise role of the FN isoforms is poorly understood. One of the alternatively spliced exons is the extra domain A (EDA) or extra type III homology that is regulated spatially and temporally during development and aging. To study its in vivo function, we generated mice devoid of EDA exon-regulated splicing. Constitutive exon inclusion was obtained by optimizing the splice sites, whereas complete exclusion was obtained after in vivo CRE-loxP–mediated deletion of the exon. Homozygous mouse strains with complete exclusion or inclusion of the EDA exon were viable and developed normally, indicating that the alternative splicing at the EDA exon is not necessary during embryonic development. Conversely, mice without the EDA exon in the FN protein displayed abnormal skin wound healing, whereas mice having constitutive inclusion of the EDA exon showed a major decrease in the FN levels in all tissues. Moreover, both mutant mouse strains have a significantly shorter lifespan than the control mice, suggesting that EDA splicing regulation is necessary for efficient long-term maintenance of biological functions.

Introduction

Fibronectins (FNs)* are high molecular weight glycoproteins that are present on many cell surfaces, in extracellular fluids, connective tissues, and basement membranes. They interact with other ECM proteins and cellular ligands, such as glycosaminoglycans, collagen, fibrin, and integrins (Kornblihtt and Gutman, 1988; Hynes, 1990). FNs play key roles in the adhesive and migratory behavior of cells related to fundamental processes such as embryogenesis, malignancy, hemostasis, wound healing, host defense, and maintenance of tissue integrity (Hynes, 1990; ffrench-Constant, 1995; Kornblihtt et al., 1996). FN molecules are a mixture of several protein types that differ in both their primary structure and post-translational modifications. The amino acid sequence variations are the consequence of the alternative processing of a single primary transcript at three sites: extra domain B (EDB) or extra type III homology B (also called EIII-B or EDII), extra domain A (EDA [EIII-A or EDI]) and type III homologies connecting segment (IIICS; V region in rat). The alternative splicing process is cell type-, developmentally, and age regulated. The EDA and EDB are single exons coding for single type III repeats that are included or excluded from the FN mRNA by exon skipping (Kornblihtt et al., 1984; Gutman and Kornblihtt, 1987; Schwarzbauer et al., 1987; Zardi et al., 1987). The IIICS region undergoes a more complex pattern of splicing which is species dependent (Schwarzbauer et al., 1983). In humans, over 20 main different isoforms are generated after mRNA processing, whereas in rats and mice, 12 variants are produced (ffrench-Constant, 1995; Kornblihtt et al., 1996). Two major forms of FN exist, plasma (pFN)

A.F. Muro and A.K. Chauhan contributed equally to this work.

The online version of this article includes supplemental material.

Address correspondence to Francisco E. Baralle, International Center for Genetic Engineering and Biotechnology (ICGEB), Padriciano 99, 34012 Trieste, Italy. Tel.: (39) 040-375-7337. Fax: (39) 040-226555. E-mail: baralle@icgeb.trieste.it

*Abbreviations used in this paper: IIICS, type III homologies connecting segment; EDA, extra domain A; EDB, extra domain B; ES, embryonic stem; cFN, cellular FN; FN, fibronectin; MEF, mouse embryonic fibroblasts; MMP, matrix metalloproteinases; p.c., postcoitus; pFN, plasma FN.

Key words: ECM; integrin receptors; basal lamina; aging; CRE-loxP

and cellular (cFN), having similar but not identical polypeptides of ~220–240 kD. pFN is a soluble dimeric form that lacks both the EDA and EDB domains. It is synthesized by hepatocytes and secreted into the bloodstream. cFN is a dimeric or cross-linked multimeric form containing the EDA and EDB domains at variable proportions. It is made by fibroblasts, epithelial, and other cell types, and is deposited as fibrils in the ECM (Hynes, 1990; ffrench-Constant, 1995; Kornblihtt et al., 1996).

The molecular mechanisms involved in processing the FN transcript are well understood for both the EDA and EDB exons (Mardon et al., 1987; Lavigueur et al., 1993; Caputi et al., 1994; Du et al., 1997; Lim and Sharp, 1998; Muro et al., 1999). The mouse EDA exon is regulated in a similar manner to its human counterpart and optimization of the 5′ and 3′ splice junctions of the exon leads to constitutive splicing in NIH3T3 cells (Muro et al., 1998).

Despite the fact that both FN primary structure and FN alternative splicing were described almost two decades ago (Kornblihtt et al., 1983; Petersen et al., 1983; Schwarzbauer et al., 1983; Kornblihtt et al., 1984; Zardi et al., 1987), many aspects of the function of FN isoforms remain elusive. In vivo studies in chicken, rat, and *Xenopus* showed the increased inclusion of EDA and EDB exons in the FN mRNA derived from embryos during development (ffrench-Constant and Hynes, 1989; Oyama et al., 1989; Pagani et al., 1991; DeSimone et al., 1992). Once development is complete, the inclusion of EDA and EDB decreases in a wide range of tissues. In fact, EDA^- and EDB^- forms are the most abundant forms in adult humans and rats (Magnuson et al., 1991; Pagani et al., 1991). This exclusion is cell type specific and differs in extent between the two exons. Quantitative mRNA studies in these tissues showed that the EDB exon is excluded more often than the EDA exon from the FN mRNA (ffrench-Constant and Hynes, 1989; Pagani et al., 1991; Caputi et al., 1995). It has been postulated that the inclusion of the spliced regions could alter the conformation of the RGD sequence, which is the main cell-binding site, via modification of its neighboring modules (ffrench-Constant, 1995) or by the alteration of the global conformation of the FN molecule (Manabe et al., 1997). In both cases, the alteration might affect the strength of the central cell–binding domain interaction with integrins. Since integrins $\alpha_9\beta_1$ and $\alpha_4\beta_1$ were recently described as the cellular receptors for the EDA segment, another possibility is that cell adhesion can be directly regulated by alternative splicing (Liao et al., 2002). Other functions proposed for the EDA segment are as follows: wound healing (Clark et al., 1983; ffrench-Constant et al., 1989); matrix assembly (Guan et al., 1990); dimer formation (Peters et al., 1990); secretion (Wang et al., 1991); cell adhesion (Xia and Culp, 1995); cell differentiation (Jarnagin et al., 1994); tissue injury and inflammation (Satoi et al., 1999; Okamura et al., 2001); and cell cycle progression and mitogenic signal transduction (Manabe et al., 1999). Because most of the above studies were done using in vitro and cell culture systems, the in vivo role of the EDA segment still remains obscure. The use of mouse models could provide the best approach to understand the in vivo function of the EDA exon. However, the in vivo study of the function of the different protein isoforms is complex due to the simultaneous presence of more than one protein form at a given specific developmental time and tissue. Gene targeting in mice has allowed the specific deletion of alternatively spliced exons in different protein systems such as α_6 integrin, γ-aminobutyrate receptor, dopamine D2 receptor, FN, Pax6, and Stat3 (Gimond et al., 1998; Homanics et al., 1999; Usiello et al., 2000; Wang et al., 2000; Fukuda et al., 2002; Singh et al., 2002; Yoo et al., 2002). Thus, it represents the best approach to understand the in vivo function of the EDA exon.

Taking advantage of our detailed knowledge of the elements involved in EDA splicing regulation (Mardon et al., 1987; Caputi et al., 1994; Muro et al., 1998, 1999), we have designed a novel approach to study the in vivo function of protein isoforms coded by genes that undergo alternative splicing without modifying the coding sequence of the FN gene. Using gene targeting, we generated a mouse strain containing the EDA allele with optimized splice sites at both splicing junctions (EDA^+ allele), with loxP sites located in the adjacent introns. By mating this mouse strain with a "deleter" CRE-recombinase expressing mouse, an EDA-null allele was obtained (EDA^- allele). Here, we show that FN mRNA produced by homozygous $EDA^{+/+}$ mice contained constitutive inclusion of the EDA exon devoid of developmental and tissue-specific regulation. Mice lacking EDA splicing regulation ($EDA^{+/+}$ and $EDA^{-/-}$) were viable and phenotypically similar to the wild-type mice. However, the mouse strain producing EDA^- FN showed an abnormal cutaneous skin wound healing. On the other hand, mice having the EDA exon constitutively included in the FN mRNA showed normal wound healing but had a striking decrease in the levels of FN in most of the organs analyzed from adult mice. Furthermore, and most importantly, both mouse strains had a significantly shorter lifespan than $EDA^{wt/wt}$ animals, suggesting that the presence of both isoforms was necessary for efficient long-term maintenance of biological functions.

Results

The study of the in vivo function of protein isoforms generated by alternatively spliced genes is generally limited by the fact that the different isoforms coexist in a temporal and spatial manner in the same tissue of the organisms. Therefore, the availability of animal models having a controlled expression of the different forms is crucial for these studies.

We have previously reported that optimization of the 5′ and 3′ splicing sites of the mouse EDA exon from the FN gene leads to constitutive exon inclusion in NIH3T3 cells (Muro et al., 1998). These results coupled with the power of homologous recombination technology in mouse embryonic stem (ES) cells enabled us to study the biological significance of protein isoforms generated by alternative splicing (for a detailed description of the rationale see Online supplemental material available at http://www.jcb.org/cgi/content/full/jcb.200212079/DC1). Furthermore, to date, there is no report of optimization of splice sites leading to constitutive splicing in vivo of a natural alternatively spliced exon.

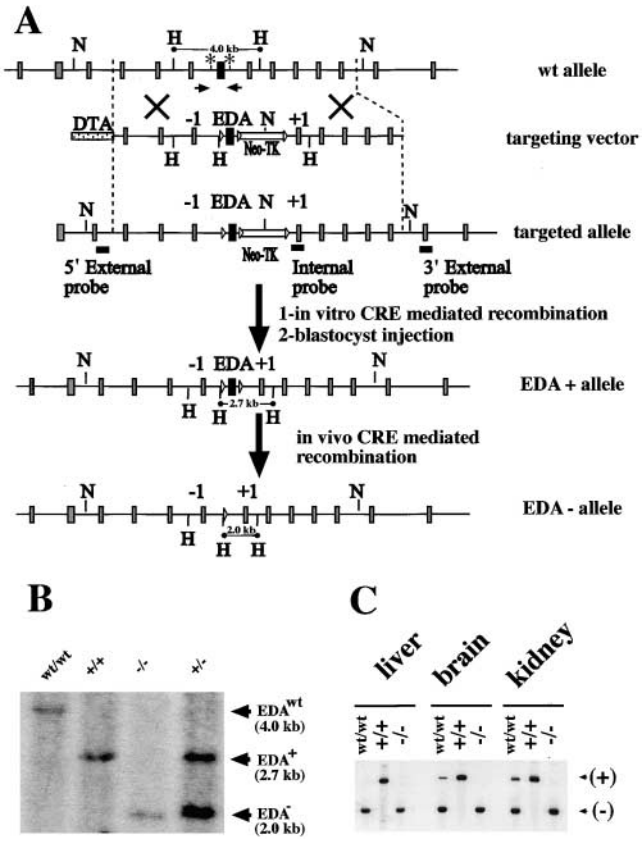

Figure 1. **Strategy for the generation of mouse strains lacking regulated splicing at the EDA exon of the FN gene.** (A) Partial maps of the wild-type FN allele, the targeting vector, the targeted allele, the EDA-floxed allele, and the EDA-null alleles. Exons, Neo-TK, and DTA are shown as gray, white, and dotted boxes, respectively. The EDA exon and the "loxP" sites are indicated as a black square and as white triangles, respectively. N and H indicate NcoI and HindIII sites, respectively. The recombinant ES cells were transiently transfected with a CRE-recombinase expressing plasmid, and $EDA^{+/wt}$ heterozygote cells were used for blastocyst microinjection. $EDA^{+/wt}$ mice were mated with a CRE-expressing transgenic mouse strain to obtain the $EDA^{-/wt}$ mice. The asterisks indicate the NdeI sites. The 4.0-, 2.7-, and 2.0-kb DNA fragments (EDA^{wt}, EDA^{+}, and EDA^{-} alleles, respectively) obtained after digestion with HindIII and Southern blot hybridization with the internal probe are indicated. (B) Southern blot screening of the different mouse genotypes. EDA^{wt}, EDA^{+}, and EDA^{-} bands are indicated. (C) RT-PCR analysis of total RNA prepared from $EDA^{wt/wt}$, $EDA^{+/+}$, and $EDA^{-/-}$ from liver, brain, and kidney is shown. EDA^{+} and EDA^{-} bands are indicated (805 and 535 bp, respectively).

Mouse strains lacking alternative splicing at the EDA exon develop normally and are fertile

To generate an FN allele devoid of alternative splicing in the EDA exon, the wild-type EDA exon in the FN gene was replaced with a "floxed" EDA exon having both the 5′ and 3′ optimized splice sites described in Fig. S1 (available at http:www.jcb.org/cgi/content/full/jcb.200212079/DC1). After electroporation of 129 Sv/J ES cells with the targeting construct (Fig. 1 A), G418-resistant clones were selected and analyzed by Southern blot hybridization. A second step of recombination by transient expression of the CRE-recombinase was performed to eliminate the Neo-TK cassette from the EDA-flanking intron. Southern blot analysis and sequencing of the PCR-amplified genomic EDA region confirmed the introduction of the optimized 3′ and 5′ splice sites and the loxP sites flanking the EDA exon in one of the FN alleles. Hereafter, this allele will be called the EDA^{+} allele. The heterozygous $EDA^{+/wt}$ ES cells were used to obtain male chimeras that transmitted the EDA^{+} allele to the germline. Heterozygous $EDA^{+/wt}$ mice were mated with CMV-CRE-transgenic mice to obtain the EDA-null allele (henceforth, called the EDA^{-} allele) after in vivo deletion of the loxP-flanked EDA exon. Homozygous mice were obtained by interbreeding heterozygous mice, and screening was performed by Southern blot analysis (Fig. 1 B) or by PCR of tail DNA biopsies (not depicted).

The homozygous $EDA^{+/+}$ and $EDA^{-/-}$ mice after birth exhibited no apparent developmental abnormalities compared with wild-type or heterozygous littermates; they reached adulthood and were fertile. In addition, no differences were detected in the organs from homozygous $EDA^{+/+}$ and $EDA^{-/-}$ mice by gross histological and pathological analysis (unpublished data). The mutated alleles segregated at the expected Mendelian frequency, and litter size and survival rate of newborn mice (measured until weaning of the litter) were similar to that of $EDA^{wt/wt}$ animals. No differences were observed neither in the shape of the embryos nor in the number of somites of embryos derived from timed matings. The detailed data are shown in the Online supplemental material section.

$EDA^{+/+}$ mice lack alternative splicing of the EDA exon

The inclusion of the EDA exon within the FN mRNA is subjected to a tight tissue-specific regulation. The most dramatic example is seen in liver, where pFN is synthesized and the EDA exon is completely excluded from the mRNA in the adult (Tamkun and Hynes, 1983; Kornblihtt et al., 1984).

Radioactive RT-PCR was used to analyze most of the tissues and organs in all three genotypes ($EDA^{wt/wt}$, $EDA^{+/+}$, and $EDA^{-/-}$). An example of the EDA splicing pattern in representative tissues such as liver, brain, and kidney is shown in Fig. 1 C. These results were confirmed by RNase protection analysis of the same samples (Fig. S2 available at http:www.jcb.org/cgi/content/full/jcb.200212079/DC1). We observed that the EDA^{+} form was never present in the samples from $EDA^{-/-}$ mice and the EDA^{+} product from $EDA^{+/+}$ mice was present in all tissues. Both RNase protection and RT-PCR analysis of the FN mRNAs showed that there is 99–100% inclusion of the EDA exon in all tissues from $EDA^{+/+}$ mice, whereas there is 100% EDA exon exclusion in all tissues belonging to the $EDA^{-/-}$ mice. This confirmed that the rationale of genetic modification was successfully fulfilled in the real in vivo situation.

Normal FN-ECM formation in mouse embryonic fibroblasts (MEF) derived from mice lacking regulated splicing at the EDA exon

Next, we examined the expression of FN mRNA, protein isoforms and ECM formation in MEF prepared from $EDA^{wt/wt}$, $EDA^{+/+}$, and $EDA^{-/-}$ animals. RT-PCR analysis confirmed the constitutive splicing-in of the EDA exon in the $EDA^{+/+}$ and its absence in the $EDA^{-/-}$ MEFs (Fig. 2 A). Analysis of protein extracts by Western blot using polyclonal anti-FN

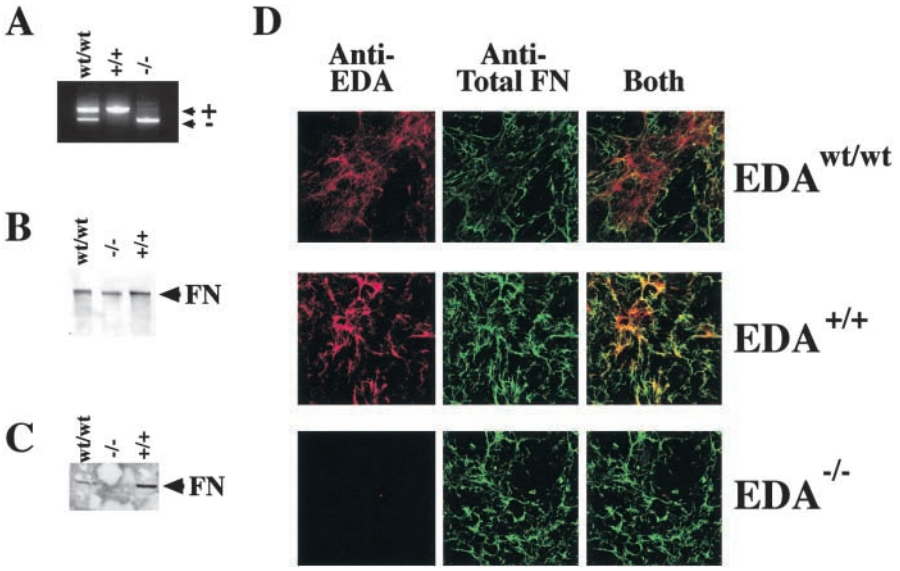

Figure 2. **Regulated splicing of the EDA is dispensable for the ECM formation.** (A) RT-PCR analysis of total RNA prepared from MEF from EDA$^{wt/wt}$, EDA$^{+/+}$, and EDA$^{-/-}$ embryos (13.5 d postcoitus [p.c.]). (B and C) Western blot analysis of protein extracts prepared from the above-described MEF (20 and 100 μg for B and C, respectively) with anti-FN and anti-EDA antibodies, respectively. Coomassie blue staining showed equal loading. (D) MEF prepared from EDA$^{wt/wt}$, EDA$^{+/+}$, and EDA$^{-/-}$ embryos (13.5 d p.c.) were plated, fixed, and incubated with anti-EDA antibody (left column) or with anti–total FN antibody (middle column). The merged image is shown in the right column.

and monoclonal anti-EDA antibodies showed normal protein levels in both the EDA$^{+/+}$ and EDA$^{-/-}$ MEF (Fig. 2 B). The anti-EDA antibody detected the EDA^{+} FN isoform only in EDA$^{+/+}$ and EDA$^{wt/wt}$ MEF (Fig. 2 C).

Immunofluorescence analysis using a confocal microscope showed the presence of a normal FN-ECM in EDA$^{+/+}$ and EDA$^{-/-}$ MEF when compared with EDA$^{wt/wt}$ MEF (Fig. 2 D). The signal obtained with the anti-EDA antibody colocalized with that observed with the anti-FN antibody.

Ablation of regulated splicing in the EDA exon produced a decrease in FN levels in EDA$^{+/+}$ mice that did not correlate to changes neither in FN mRNA nor in the integrin levels

Next, we examined whether the modifications in the natural alternative splicing pattern of FN had some consequences in other cellular proteins or FN itself. Consequently, protein extracts from different tissues of the different genotypes were

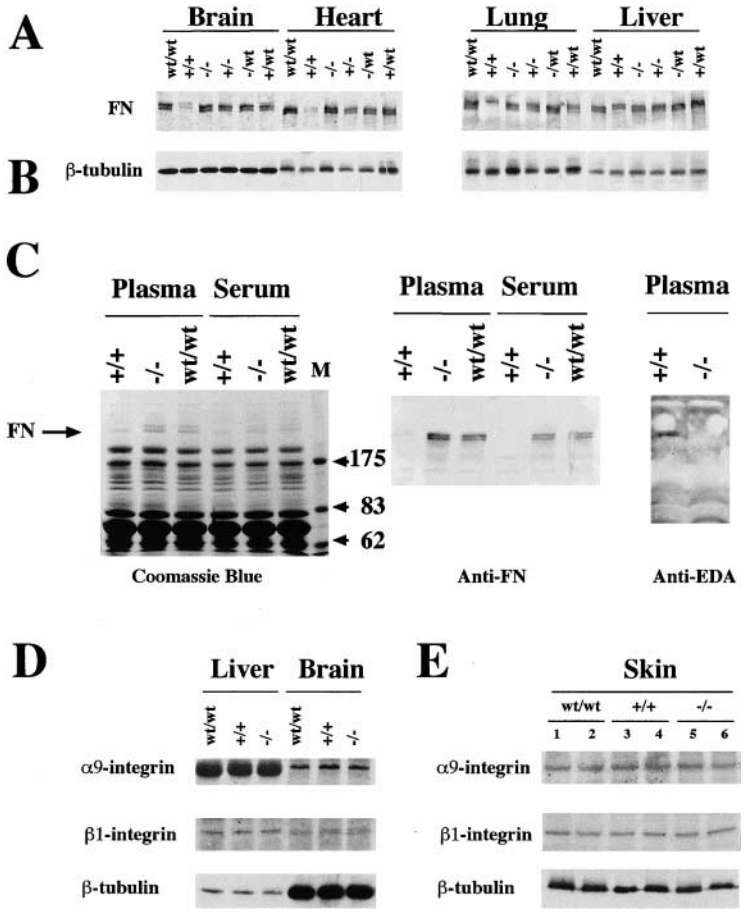

Figure 3. **The decrease in FN levels in tissues of EDA$^{+/+}$ mice is not correlated to a reduction in integrin levels.** (A and B) Western blot analysis of total protein extracts (50 μg) from brain, heart, lung, and liver from all genotypes (EDA$^{wt/wt}$, EDA$^{+/+}$, EDA$^{-/-}$, EDA$^{+/-}$, EDA$^{-/wt}$, and EDA$^{+/wt}$) using anti-FN polyclonal antibody (A) and, after stripping the membrane, anti–β-tubulin mAb to verify for minor errors in protein load (B). Note that the migration of the EDA^{+} FN is slightly slower than that of the EDA^{-} FN. Coomassie blue staining of 5–17% gradient gels of the same protein extracts did not show changes in other proteins. (C) Plasma and serum protein samples from EDA$^{+/+}$, EDA$^{-/-}$, and EDA$^{wt/wt}$ mice (20 μg) were Coomassie blue stained (left), and a similar gel was blotted and incubated with anti-FN antibody (middle). For the anti-EDA antibody (right), 100 μg of protein extract were loaded. (D and E) Western blot analysis of α_9- and β_1-integrin levels in different tissues (liver, brain, and skin) using anti-α_9 and -β_1 rabbit polyclonal antibodies. Anti–β-tubulin mAb was used to verify for minor errors in protein load.

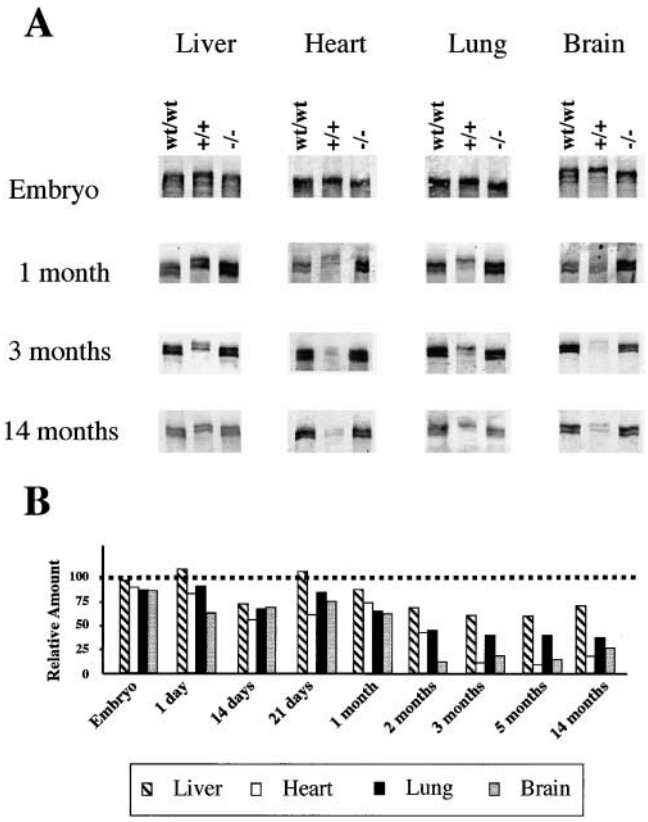

Figure 4. **Expression of FN in different tissues at different ages.** (A) Protein extracts from liver, heart, lung, and brain were prepared from $EDA^{wt/wt}$, $EDA^{+/+}$, and $EDA^{-/-}$ mice of different ages (13.5 d p.c., 1, 3, and 14 mo old) and analyzed by Western blot using an anti-FN antibody. (B) The histograms represent the relative amount of FN present in $EDA^{+/+}$ mice relative to that present in $EDA^{wt/wt}$ mice (considered as 100%) for each tissue and each time point.

prepared from 3-mo-old mice and analyzed by SDS-PAGE. No evident difference was observed at least at the sensitivity level of Coomassie blue staining of 5–17% gradient gels (unpublished data). On the other hand, a Western blot analysis using anti-FN polyclonal antibody showed a striking decrease in FN levels in most of the tissues analyzed from $EDA^{+/+}$ mice (Fig. 3 A). This decrease was also evident in $EDA^{+/wt}$ and $EDA^{+/-}$ mice, both bearing one EDA^{+} allele. The observed differences were not due to a different protein load of the gels, as evidenced by the Coomassie blue staining and by the incubation of the same membranes with an anti–β-tubulin mAb (Fig. 3 B). A significant decrease in FN amounts was also observed in the plasma and serum samples prepared from $EDA^{+/+}$ animals when compared with those from $EDA^{wt/wt}$ mice (Fig. 3 C). Western blot using an anti-EDA antibody confirmed the presence of EDA containing FN in the $EDA^{+/+}$ plasma and its complete absence in the $EDA^{-/-}$ sample (Fig. 3 C).

It was considered important to analyze if the FN level differences observed in the different tissues were associated to changes in the levels of the specific EDA receptor $\alpha_9\beta_1$-integrin (Liao et al., 2002). We observed no differences in α_9- and β_1-integrin levels among $EDA^{wt/wt}$, $EDA^{+/+}$, and $EDA^{-/-}$ mice by Western blot analysis in liver and brain (Fig. 3 D). However, it remains to be seen if the localization pattern of the integrin receptors or their signaling have been affected in the mutant mice.

On the other hand, to determine whether the observed decrease in FN protein levels in the $EDA^{+/+}$ mice was correlated to a decrease in the mRNA levels, we performed Northern blot analysis of total RNA isolated from the tissues having the higher decrease in FN levels (brain and heart) from 3-mo-old male mice. No significant variations were

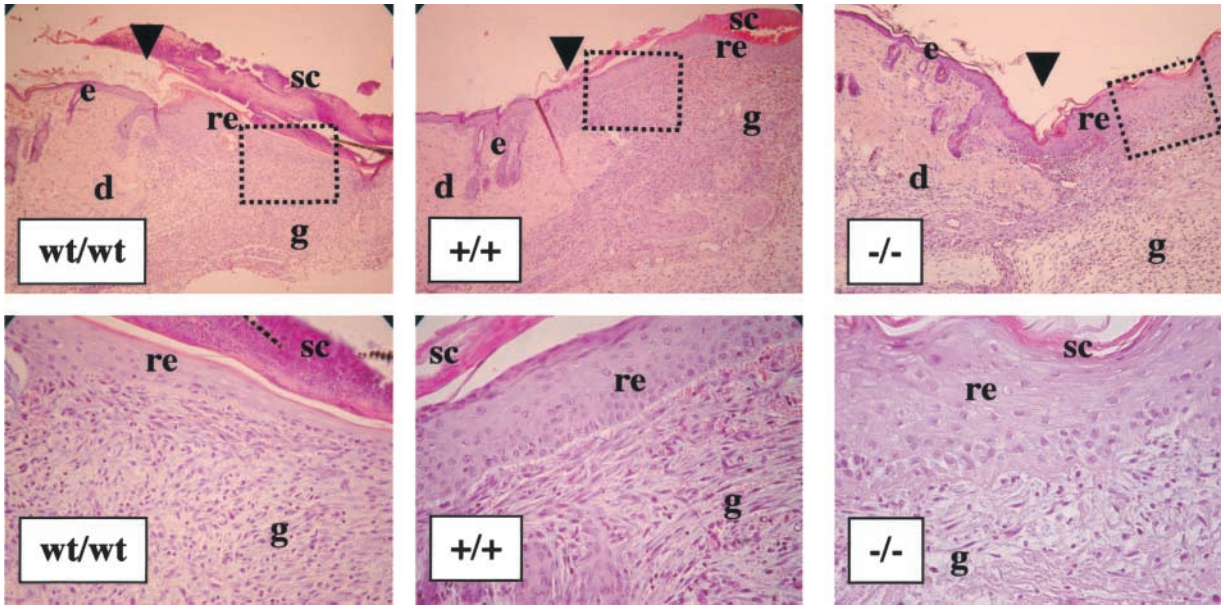

Figure 5. **Reepithelization is observed 5 d after full thickness cutaneous wounding.** Full thickness cutaneous wounds of control ($EDA^{wt/wt}$, $n = 6$) and mutant mice ($EDA^{+/+}$ and $EDA^{-/-}$, $n = 6$ and 7, respectively) mice were analyzed at 5 d after wounding by hematoxylin-eosin staining. Representative sections are shown. The black arrowheads indicate the wound edges. Epithelium, granulation tissue, dermis, newly formed epithelium, and eschar are indicated ("e," "g," "d," "re", and "sc," respectively). The dotted rectangles in the top panels indicate the magnified area showed in the bottom panels. The experiment was repeated twice with similar results. Edematous granulation tissue is observed in the $EDA^{-/-}$ wounds.

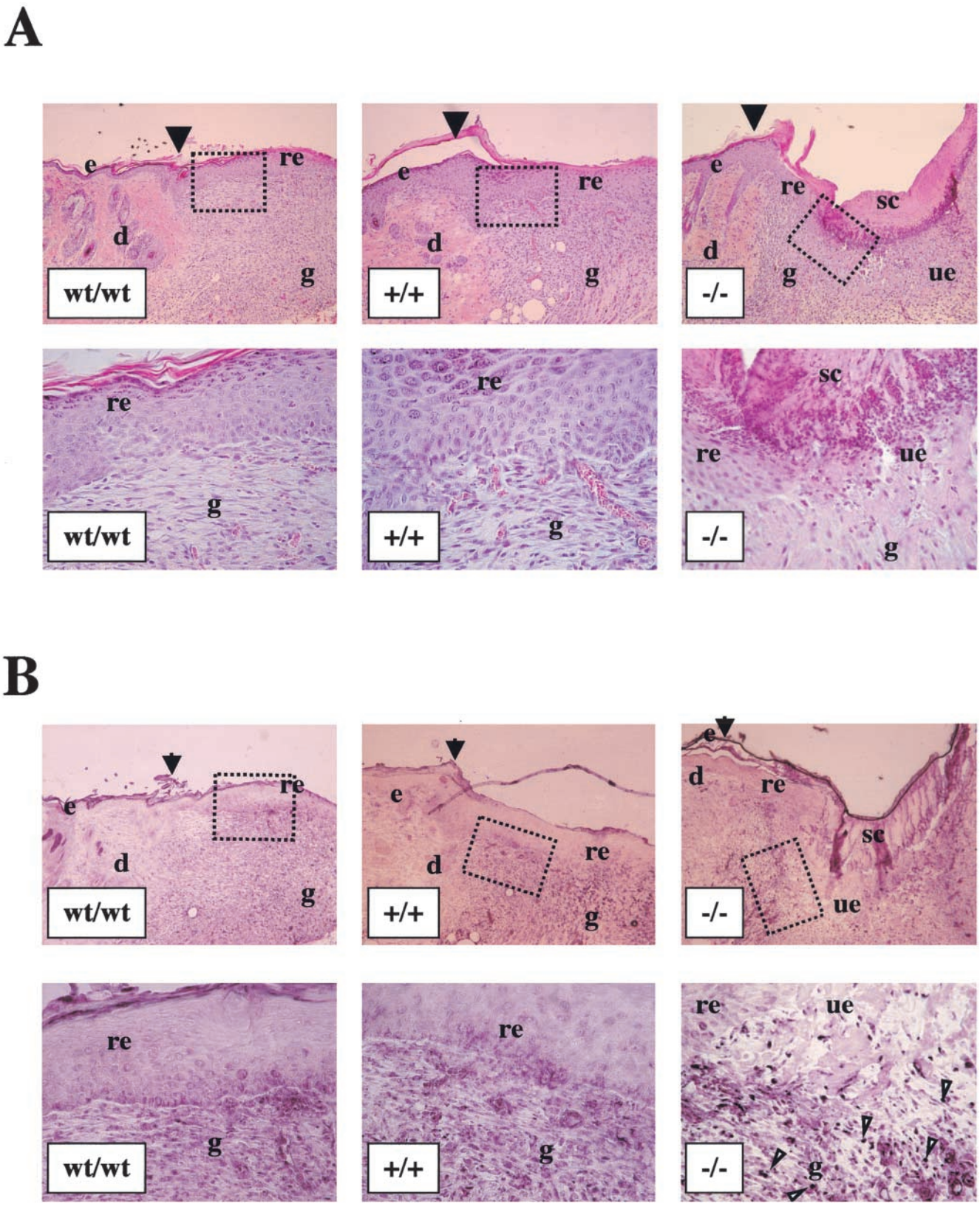

Figure 6. **EDA$^{-/-}$ skin wounds at day 7 after wounding show abnormal healing and increased number of BrdU-positive cells.** (A) Full thickness cutaneous wounds of control (EDA$^{wt/wt}$, $n = 8$) and mutant mice (EDA$^{+/+}$ and EDA$^{-/-}$, $n = 8$ and 9, respectively) mice were analyzed at 7 d after wounding. Representative sections are shown. The black arrowheads indicate the wound edges. Abbreviations are as described in Fig. 5. The ulcerated epithelium observed in the EDA$^{-/-}$ wound is indicated as "ue." The experiment was repeated three times with similar results. Wound sections of three independent experiments (eight mice per genotype in each experiments) were microscopically scored for the presence of ulcerative processes at day 7 after wounding. The fraction of ulcerated wounds of the EDA$^{-/-}$ mice was statistically significant different from that of EDA$^{wt/wt}$ and EDA$^{+/+}$ mice (63 and 22% for EDA$^{-/-}$ and EDA$^{wt/wt}$, respectively; $P < 0.0002$ for EDA$^{-/-}$ vs. EDA$^{wt/wt}$ by both

observed in RNA samples from the brain and heart of $EDA^{+/+}$ mice (Fig. S3 available at http://www.jcb.org/cgi/content/full/jcb.200212079/DC1).

Embryos and prepubertal $EDA^{+/+}$ mice have normal FN levels

To determine whether the mechanisms that produced the FN decrease were developmentally regulated, we performed a Western blot analysis of samples prepared from mice of different ages. The decrease in FN levels was not present during embryonic development. It started after birth in most of the tissues, and arrived to a plateau in 2-mo-old mice (Fig. 4). In some tissues, the FN levels in $EDA^{+/+}$ mice were ~10–20% of the amount found in $EDA^{wt/wt}$ mice (heart, blood, brain, kidney, and diaphragm), whereas the liver showed a lesser decrease in FN levels in $EDA^{+/+}$ mice, arriving to 60–70% of the amount present in $EDA^{wt/wt}$ mice.

In an attempt to determine alterations in the FN-degradative mechanisms, we performed gelatin zymography and observed no variations in plasma and other tissues (brain and heart) in the levels of matrix metalloproteinases (MMPs), enzymes known to degrade FN (Sternlicht and Werb, 2001). Moreover, no differences were observed in the degradation of in vitro translated recombinant fragments of FN with or without the EDA exon that were incubated with tissue extracts (unpublished data). Western blot analysis of tissue extracts using a polyclonal anti-FN antibody did not reveal the presence of extra bands or any smaller degradation product of $EDA^{+/+}$ tissues, neither with a 6% nor a 12% SDS-PAGE gel (unpublished data). Additionally, we were unable to reproduce in vitro the reduction in FN levels after culturing heart fibroblasts of adult mice (from 2-, 4-, and 6-mo-old animals), as the cell extracts from $EDA^{+/+}$ mice showed similar levels of FN to those of the $EDA^{wt/wt}$ fibroblasts (unpublished data).

These experiments showed that the striking reduction in FN protein levels in $EDA^{+/+}$ mice occurred after birth. The decrease in FN was not related to the mRNA levels present in each tissue or to a detectable EDA^{+}-dependent degradation, suggesting that alternative mechanisms should be responsible for the decrease of tissue FN in the $EDA^{+/+}$ animals.

EDA-null mice have abnormal skin wound healing

The FN present in the skin of wild-type animals does not contain the EDA exon. However, the FN-EDA^{+} form is thought to participate actively in the reepithelization process (Clark et al., 1983; ffrench-Constant et al., 1989). To explore the role of the EDA exon in the wound healing process, we performed full thickness excisional skin wounds in $EDA^{wt/wt}$, $EDA^{-/-}$, and $EDA^{+/+}$ mice. The wound healing process was analyzed at 1, 3, 5, 7, 10, and 14 d after wounding. Hematoxylin-eosin staining of tissues from full thickness wounds during the early phase of reepithelization (days 1 and 3) did not show any differences in reepithelization and neovascularization (unpublished data). During late phase (days 5 and 7), the reepithelization and formation of granulation tissue were indistinguishable between $EDA^{+/+}$ and $EDA^{wt/wt}$ mice (Figs. 5 and 6). However, the abnormal healing process was observed in the $EDA^{-/-}$ mice. In fact, at day 5, the newly formed epidermis completely covered the wound area in the $EDA^{-/-}$ mice but the border between the new epidermis and the granulation tissue was not sharply defined as in the control or $EDA^{+/+}$ mice. Moreover, the granulation tissue of the $EDA^{-/-}$ wounds showed less compact cells with edematous-like areas below the interface between the epidermis and the derma granulomatous reaction (Fig. 5, bottom).

At day 7, the $EDA^{-/-}$ wounds were clearly different from those from $EDA^{wt/wt}$ and $EDA^{+/+}$ mice (Fig. 6 A, bottom). In fact, the $EDA^{-/-}$ wounds showed ulcerative processes at the newly formed epidermal region level, resulting in a delay in the reepithelization. Infiltration of inflammatory cells such as polymorphonuclear leukocytes and macrophages were detected by microscopic analysis of the edematous-like and ulcerative regions, and a higher cell proliferative activity was observed by in vivo BrdU labeling in these regions (Fig. 6 B, bottom right). On the contrary, neither $EDA^{wt/wt}$ nor $EDA^{+/+}$ wounds presented a high number of BrdU-positive cells in the area below the newly formed epidermal region (Fig. 6 B, bottom left and center). The status of the basal lamina in the $EDA^{-/-}$ skin was similar to that of the $EDA^{wt/wt}$, as seen by both the Azan-Mallory coloration and the specific staining of laminin in the same sections using a rabbit polyclonal antilaminin antibody. Cell death and apoptosis-specific analysis were performed by TUNEL and caspase-3 assays of the wound sections, respectively, and showed no significant differences in the number of positive cells between the different genotypes (Fig. S4 available at http://www.jcb.org/cgi/content/full/jcb.200212079/DC1). Scoring of the skin healing process of three independent experiments (eight 3-mo-old mice per genotype in each experiment) for the presence of ulceration in the wounds showed that $EDA^{-/-}$ mice developed them 2.9 times more frequently than the $EDA^{wt/wt}$ mice (63% of $EDA^{-/-}$ vs. 22% of $EDA^{wt/wt}$, $P < 0.0002$ by both the Fisher Exact test and the χ^2 test) at d 7 after wounding.

A limited number of 11-mo-old mice (five $EDA^{wt/wt}$ and six $EDA^{-/-}$mice) that were subjected to the same wound healing protocol showed an even higher proportion in the frequency of wound ulceration in the $EDA^{-/-}$ mice (83.3% vs. 20%, $EDA^{-/-}$ and $EDA^{wt/wt}$; respectively. $P \leq 0.01$ by both the Fisher Exact test and the χ^2 test).

To determine whether integrin $\alpha_9\beta_1$ levels were changed, we performed a Western blot analysis of untreated skin samples and observed similar levels of integrin $\alpha_9\beta_1$ among all three genotypes (Fig. 3 E).

the Fisher Exact test and the χ^2 test). There were no differences between the $EDA^{wt/wt}$ and $EDA^{+/+}$ scores). (B) BrdU labeling shows an increased number of replicating cells in the $EDA^{-/-}$ wounds. Serial sections of the same wounds seen in A were incubated with an anti-BrdU mAb. The count of several microscopical fields showed that there are at least 10 times more BrdU-positive nuclei in the area below the newly formed epidermis in the $EDA^{-/-}$ wounds when compared with $EDA^{wt/wt}$ or $EDA^{+/+}$ wounds. A representative field is shown. More than 50 positive nuclei are observed in the $EDA^{-/-}$ wound (bottom right), whereas less than five positive nuclei are observed in the case of $EDA^{wt/wt}$ or $EDA^{+/+}$ samples (bottom left and center, respectively). Illustrative BrdU-labeled nuclei are indicated by white triangles. The black arrows indicate the wound edges.

Constitutive exclusion or inclusion of the EDA exon within the FN mRNA shortens the lifespan

The in vivo studies performed on rats show a critical decrease in EDA^+/EDA^- ratio after birth, with an additional gradual decrease of the ratio in some tissues that is correlated with the age of the animal (Magnuson et al., 1991; Pagani et al., 1991). We addressed the question if in $EDA^{+/+}$ and $EDA^{-/-}$ mice, having no regulation of EDA splicing, the presence or absence of the EDA exon could have an effect on their lifespan. For this purpose, we performed a long-term experiment using 139 mice ($EDA^{wt/wt}$, $n = 39$; $EDA^{+/+}$, $n = 47$; and $EDA^{-/-}$ $n = 53$) that were caged separately throughout the experiment and the time of animal death was recorded. The Kaplan-Meier graphical representation of the data is shown in Fig. 7. It can be seen that up to 15-mo-old mice from all the genotypes did not show any difference in survival. However, from thereon, there was a decline in the survival rate in $EDA^{+/+}$ and $EDA^{-/-}$ mice. At 30 mo, only seven and eight $EDA^{+/+}$ and $EDA^{-/-}$ mice were alive, (10 and 12.5% survival, respectively), whereas 21 $EDA^{wt/wt}$ mice survived (53.8% survival). Log-rank test statistical analysis indicated that both $EDA^{+/+}$ and $EDA^{-/-}$ mice lifespan curves were statistically significant when compared with $EDA^{wt/wt}$ mice with $P \leq 0.0005$. Postmortem external examination showed that 20–25% of the $EDA^{-/-}$ mice had different skin hyperproliferative and spontaneous ulcerative lesions on their mid-dorsal skin. In case of the $EDA^{wt/wt}$ and $EDA^{+/+}$ mice, <5% had any kind of skin lesions. Autopsies were performed on naturally deceased mice of all three genotypes. Liver tumors, intestinal obstruction, prostatic necrosis, and pulmonary edema were the most frequently observed features, but there was no significant difference in these pathologies of the internal organs between the three genotypes.

Discussion

The first evidence of the in vivo importance of FN was demonstrated by R. Hynes's group who showed that FN-null mice die during embryonic development (George et al., 1993). The early embryo lethality makes it difficult to study the biological functions of FN in the in vivo models. Therefore, one of the best methodologies to study the function of FN is by selective modification of the gene. Along with this line, Sakai et al. (2001) described a mouse model lacking pFN which showed increased neuronal apoptosis and larger infarction areas after transient focal cerebral ischemia. In an attempt to elucidate the role of the EDB exon, mice lacking this exon were also produced, but showed no obvious abnormalities in vivo (Fukuda et al., 2002).

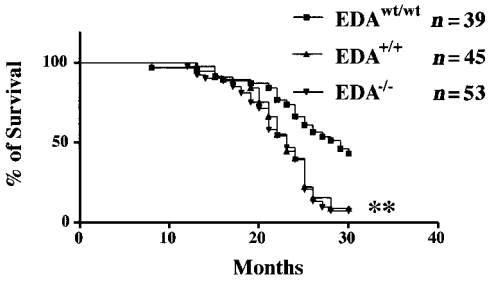

Figure 7. **The lack of alternative splicing of the EDA exon reduces the lifespan of mutant mice.** Both $EDA^{+/+}$ and $EDA^{-/-}$ mice showed a reduced lifespan during the 30-mo period of analysis. The graphic shows a Kaplan-Meier representation of the survival versus time of 39, 45, and 53 $EDA^{wt/wt}$, $EDA^{+/+}$, and $EDA^{-/-}$ mice, respectively, that were housed in individual cages throughout the study. The results were analyzed with the Log-rank test and both the $EDA^{+/+}$ and the $EDA^{-/-}$ curves were statistically significant when compared with the $EDA^{wt/wt}$ mice (indicated by asterisks, $P \leq 0.0005$).

We have investigated the in vivo role of the EDA exon by constructing mouse strains unable to carry out EDA exon alternative splicing. The $EDA^{+/+}$ strain showing constitutive expression of the EDA exon in all tissues was obtained without any modification of the coding sequences and gene structure. This novel approach avoided the difficulties found in a previous attempt to produce animals devoid of alternative splicing of the EDB exon in the FN gene where the modification of the gene structure through the introduction of a selection cassette within the introns produced an FN-null allele (Georges-Labouesse et al., 1996). A similar phenomenon has recently been observed in other genes (Lewandoski, 2001). None of these negative effects was observed in our mutant mice, indicating that the insertion of loxP sites within the flanking introns did not modify the normal pre-mRNA transcription and processing.

Moreover, we observed no obvious embryonic mortality nor malformation in any of the homozygous mutant mice analyzed ($EDA^{+/+}$ and $EDA^{-/-}$ animals), suggesting that the alternative splicing regulation of the EDA exon is not essential for the developmental processes or that it could be compensated by other gene products. The absence of any obvious developmental abnormality in $EDA^{+/+}$ and $EDA^{-/-}$ mice suggests that the information and postulated roles for the EDA exon obtained by using recombinant FN fragments (Introduction) cannot be extended automatically to the in vivo functions where more complex mechanisms are acting.

$EDA^{+/+}$ mice have decreased levels of FN in all tissues

The observation of decreased levels of FN in adult $EDA^{+/+}$ mice, but not in embryos and very young mice (<1 mo old) suggests that different control mechanisms of FN levels are acting before and after puberty. This decrease could be due to one of the following explanations or a combination of them: (1) a decrease in FN mRNA levels; (2) a decrease in the secretion rate of FN; or (3) an increase in extracellular degradation of FN.

A series of experiments have been performed to test which of these mechanisms, if any, was acting in the $EDA^{+/+}$ mice. Northern blot experiments showed that the mRNA levels were not directly related to FN protein levels (Figs. 3 and 4 and Fig. S3). Protease levels were similar to those of $EDA^{wt/wt}$, no additional FN degradation products were seen in $EDA^{+/+}$ tissue extracts, and we were unable to see a decrease of FN levels in in vitro cultured cells derived from adult organs of $EDA^{+/+}$mice. The failure to identify the precise cause of the low FN-EDA^+ levels suggests that an atypical mechanism might be acting. One possibility is that a specific intracellular trafficking mechanism is able to modulate the levels of EDA^+ FN forms in adult animals. This mechanism was suggested for polarized secretion of FN forms in airway

epithelial cells (Wang et al., 1991). It is interesting to note that Schwarzbauer et al (1989) have shown that the IIICS-0/IIICS-0 dimers were not secreted. It is possible that a similar control in the secretion mechanism could also be present for the EDA^+ subunits.

However, none of these effects was obvious in cultured fibroblasts from embryos and adult animals, and in the early stages of development of mice. In fact, the decrease in the amount of FN was evident only after 2–3 mo of age, which is after sexual development. Alternatively, a down-regulation of specific tissue inhibitors of MMPs in adult animals would have as its consequence an increase in activity of specific MMPs, a subtle change that direct gelatin zymography analysis will not detect.

Cutaneous wound healing is abnormal in $EDA^{-/-}$ mice

Initially, up to 3 d after wounding, there were no differences in the healing process between the three genotypes ($EDA^{wt/wt}$, $EDA^{-/-}$, and $EDA^{+/+}$). This seems to be consistent with the fact that in the first days after wounding, deposited FN is mainly derived from plasma (Clark et al., 1983; ffrench-Constant et al., 1989). It was shown that normal wound healing could be helped by the presence of cFN (ffrench-Constant et al., 1989; Sakai et al., 2001). In fact, in mice devoid of pFN, normal wound healing was reported (Sakai et al., 2001). cFN is produced in situ 3 d after wounding (Clark et al., 1983; ffrench-Constant et al., 1989; Sakai et al., 2001) and a thin layer of cFN deposited on the surface of the wound immediately after injury in pFN-null mice (Sakai et al., 2001). Expression of cFN by the cells found at the base and edges of the wound just beneath the epidermis was observed, and the presence of cFN preceded the migration of epithelial cells that eventually covered the wound (ffrench-Constant et al., 1989). Previous studies have also shown that FN appears in the provisional matrix beneath the migrating epidermis coordinating with the FN-receptor expression on migrating epidermal cells (Clark et al., 1982, 1983; Grinnell, 1984). These data correlate perfectly with our results showing that after that period, despite the formation of granulation tissue and neovascularization, we observed abnormal reepithelization in $EDA^{-/-}$ mice. The granulation tissue of the $EDA^{-/-}$ wounds displayed edematous regions that occur before the ulcerative process. The subsequent epidermal ulceration was accompanied by a proliferative stimulus with the influx of polymorphonuclear leukocytes and macrophages, and a delay in the healing of the wounds. Possible reasons for these phenomena could be related to defects in the basal lamina, a change in integrin receptor levels, and/or a defect in the skin keratinocytes, fibroblasts, or immune system. The basal lamina looked similar in $EDA^{-/-}$ mice compared with $EDA^{wt/wt}$ mice by both Azan-Mallory coloration and the specific immunostaining of laminin. However, we cannot rule out minor differences in one of the other specific proteins that are present in the basal lamina. Moreover, similar levels of $\alpha_9\beta_1$ integrin, one of the EDA receptors (Liao et al., 2002), were observed in skin of the three genotypes. Preliminary attempts to define differences between the $EDA^{wt/wt}$ and $EDA^{-/-}$ genotypes in immune system cells (T/B lymphocytes ratio and delayed hypersensitivity) and in the characteristics of fibroblasts (in vitro cell migration, cell adhesion, and duplication time) failed to show significant differences. However, it remains to be seen if the localization pattern of the integrin receptors or their signaling have been affected in the mutant mice.

The increase in ulceration in the $EDA^{-/-}$ wounds could be the result of a higher rate of cell death in the skin of the mice during wound closure. This does not seem to be the case as the number of positive cells between the $EDA^{wt/wt}$, $EDA^{-/-}$, and $EDA^{+/+}$ wounds in the granulation tissue were similar in the area devoid of ulceration by both TUNEL and caspase-3 assay.

On the basis of these considerations and the data described in Results, we conclude that FN containing the EDA segment plays an essential role in the organization of the granulation tissue and probably in epidermal cell migration, either directly or by interaction with other ECM components.

$EDA^{+/+}$ and $EDA^{-/-}$ mouse strains have a shorter lifespan

It has been shown that deficiency of SH2-containing inositol-5-phosphatase, lysosomal acid lipase, and DNA topoisomerase IIIβ had no consequences in embryonic development, but shortens the lifespan of the animals (Helgason et al., 1998; Du et al., 2001; Kwan and Wang, 2001). The shortened lifespan could be due to the changes in biological processes, which require the presence of the investigated protein during aging.

In the case of the FN mice, we showed that the absence of regulation of the EDA exon affects the lifespan of mutant animals. In normal animals, a dramatic change in the EDA^+/EDA^- ratio is observed after birth and a gradual decrease of EDA inclusion is observed in the tissues that increases with the age of the animal (Magnuson et al., 1991; Pagani et al., 1991). Alternative splicing of FN is regulated at both the extracellular (ffrench-Constant, 1995; Kornblihtt et al., 1996; Boyle et al., 2000) and the molecular levels (Mardon et al., 1987; Lavigueur et al., 1993; Caputi et al., 1994; Muro et al., 1999). The mutant $EDA^{+/+}$ and $EDA^{-/-}$ mice have no regulation of splicing of the EDA exon. It was possible that some biological processes that required specific EDA^+/EDA^- ratios of FN were altered because of the absence of regulation of EDA splicing. In fact, this was shown in this paper for the specific case of cutaneous wound healing in the $EDA^{-/-}$ mice. Furthermore, the low healing efficiency was exacerbated in older mice. In a similar fashion, other maintenance and tissue repair mechanisms could be affected, and the cumulative lower efficiency may result in a decrease in the lifespan of mutant animals. In the specific case of the $EDA^{+/+}$ mice, due to the dramatic reduction in FN levels in most organs, it remains unclear whether the shortened lifespan seen in $EDA^{+/+}$ mice was due to a change in FN quantity and/or quality. Although no significant differences have been reported on the lifespan of c129 and C57BL/6 (Smith et al., 1973; Goodrick, 1975; Kunstyr and Leuenberger, 1975), we cannot formally rule out that the differences in chromosome background at the FN EDA locus (C57BL/6 for the $EDA^{wt/wt}$ and c129 with one or two loxP sites for $EDA^{-/-}$ and $EDA^{+/+}$, respectively) could be responsible for the observed differences in lifespan.

In summary, we generated mice devoid of regulated splicing at the EDA exon of the FN gene. Surprisingly, both mouse strains showed that the alternative splicing at the EDA exon was dispensable during embryonic development, but it was necessary for a normal lifespan. Moreover, mice unable to incorporate the EDA exon in the FN protein displayed abnormal skin wound healing. On the other hand, mice having constitutive inclusion of the EDA exon showed an important decrease in the FN levels in all tissues.

The results presented here are important for three reasons: first, we presented a novel method to study the function of protein isoforms; second, we added valuable information regarding the function of the FN isoforms; and third, we showed that changes in the regulation of splicing are responsible for subtle changes in the phenotype that may be present, but undetected, in human pathologies.

Materials and methods

Mice

C57BL/6 mice were bred at the International Centre for Genetic Engineering and Biotechnology animal house or purchased from Harlan, Italy. All mice were housed in rooms at 25°C with 12-h light/dark cycles. Mice were fed with standard food and water ad libitum. In all experiments, mice were males and age-matched, except in the aging experiment in which both males and females were used. Blood was drawn by puncture of the internal maxillary artery.

Generation of homozygous EDA mutant mice

Cloning of the murine genomic EDA region and targeting construct. A 13-kbp genomic clone containing the EDA exon region of the murine FN gene was isolated from a 129/Sv λ DashII library (a gift of G. Friedrich, Fred Hutchinson Cancer Research Center, Seattle, WA). The exon–intron structure and restriction map of this fragment was determined by restriction enzyme mapping followed by Southern blot analysis using individual exons as probes, which were PCR amplified from the human FN cDNA. Both the 5′ and 3′ splice sites of the EDA exon were modified by PCR-directed mutagenesis as described previously (Muro et al., 1998). In brief, the 5′ splice site was mutated to the 5′ consensus (5′CAGgtaagt3′) and the 3′ splice site was replaced by that of the constitutively spliced-in second exon of the apolipoprotein AI gene, which matches exactly the 3′ consensus (see Online supplemental material).

Our targeting construct consisted of 11.5 kbp of mouse genomic DNA. Neomycin (Neo) and diphtheria toxin (DTA) genes were used as positive and negative selection markers, respectively, for the first round of recombination. Three loxP sites were included in the targeting construct flanking the Neo-Thymidine Kinase (TK) cassette and the EDA exon.

The targeting construct was electroporated into ES cells, and 350 G418-resistant clones were genotyped by Southern blot hybridization of NcoI–NdeI-digested DNA using the 5′ external probe (Fig. 1 A). Eight recombinant clones were obtained, and three of them underwent a second step of recombination by transient expression of the CRE recombinase (by transient transfection of the pBS185 plasmid; a gift of B. Sauer, Stowers Institute for Medical Research, Kansas City, MO) and selection in the presence of gancyclovir. Two recombinant clones having the deleted Neo-TK cassette and the loxP-flanked EDA were selected and amplified. More detailed Southern blot analysis and sequencing of the PCR-amplified genomic EDA region of two recombinant clones was done to confirm the introduction of the optimized 3′ and 5′ splice sites and the loxP sites flanking the EDA exon in one of the FN alleles. Both clones were used in order to obtain chimeras. Male chimeras obtained by microinjection of C57BL/6 blastocyst were mated to C57BL/6 females in order to generate heterozygous animals (F1 mice).

The F1 offsprings were analyzed for the transmission of the modified EDA exon within the FN gene. HindIII-digested DNA from tail biopsies from the agouti progeny was genotyped by Southern blot using the EDA + 1 internal probe (Fig. 1, A and B). F1 heterozygous offsprings were mated with C57BL/6 mice to obtain F2 generation, which were then mated to each other to produce $EDA^{+/+}$ mice (inclusion of the modified EDA exon in both the FN alleles). F1 $EDA^{+/wt}$ mice were mated with a CRE-recombinase transgenic mice (on a C57BL/6 background) to obtain $EDA^{-/wt}$ progeny (F2) that were subsequently mated to obtain $EDA^{-/-}$ animals.

Preparation of RNA from adult mouse and embryonic tissues

Total cellular RNA from various tissues was prepared by the guanidinium thiocyanate method (Chomczynski and Sacchi, 1987), quantitated by measuring absorbance at 260 and 280 nm, and RNA integrity was confirmed by running the samples on 1% agarose formaldehyde gels. For embryonic RNA samples, embryos were dissected under a stereomicroscope (model SMZ-10; Nikon) and tissues were pooled from five to six embryos (13.5 d p.c.). RNA was prepared using RNAZOL TM B (Biotecx Lab) according to the manufacturer's instructions.

mRNA analysis by Northern blot and radioactive RT-PCR

10–20 μg of total RNA from different tissues was denatured and run on a 1.2% agarose formaldehyde gel, blotted onto a nylon membrane (Hybond-N; Amersham Biosciences), and stained with a methylene blue solution to verify the efficiency of the transfer. The membrane was prehybridized in ExpressHyb™ hybridization solution (CLONTECH Laboratories, Inc.) and hybridized with the radioactive-labeled probe. It was exposed overnight using BIOMAX MS films (Kodak), and quantification of the radioactive signal was done with a phosphorimager (Canberra-Packard). FN cDNAs were analyzed as described in the Materials and methods section of the online supplemental material.

Preparation of protein extracts

Adult mouse tissues were surgically removed, homogenized in lysis buffer (150 mM NaCl, 50 mM Tris-HCl, pH 8, 1% wt/vol NP-40, and 2× complete protease inhibitor cocktail [Boehringer] with a polytron [Ultra-Turrax T8; Boehringer]), and analyzed by SDS-PAGE after protein determination using the Bradford assay (protein assay kit; Bio-Rad Laboratories).

In the case of embryos, tissues from five to six embryos per genotype were surgically removed with the help of a stereomicroscope and pooled. The protein extracts were prepared by sonication in 150 μl of lysis buffer.

Western blot analysis

50 μg protein extracts were run on a 6%, 12%, and a gradient of 5–17% SDS-PAGE gels. The proteins were blotted onto a nitrocellulose membrane, incubated with the first and secondary antibodies, and the reaction was developed using the ECL system (Amersham Biosciences). The following primary antibodies were used: anti–human FN goat polyclonal antibody (Sigma-Aldrich), anti–human EDA mouse mAb 3E2 (Sigma-Aldrich), anti–α_9-integrin rabbit polyclonal (a gift from D. Sheppard, University of San Francisco, San Francisco, CA), anti–β1-integrin rabbit polyclonal (Santa Cruz Biotechnology, Inc.), and the anti–β-tubulin mAb E7 (Developmental Studies Hybridoma Bank, University of Iowa) antibodies. Densitometry analysis was performed by using the Versa-Doc Analyzer (Bio-Rad Laboratories) with Quantity One software (Version 4; Bio-Rad Laboratories).

Immunofluorescence studies of MEF

Embryonic fibroblasts (13.5 d) from $EDA^{wt/wt}$, $EDA^{+/+}$, and $EDA^{-/-}$ mice were cultured on coverslips for 24 h. Cells were washed and fixed with 4% vol/vol PFA in PBS, permeabilized with 0.5% vol/vol Triton X-100 in PBS, and blocked. Cells were incubated with anti–human FN goat polyclonal antibody and in parallel with goat normal serum or with the mAb 3E2, and incubated with fluorescein-labeled rabbit anti–goat IgG (DakoCytomation) or with rhodamine-labeled rabbit anti–mouse IgG (DakoCytomation), respectively. Negative controls were performed with cells incubated directly with the fluorescent antibody. The analysis of the immunofluorescence was done by using a confocal laser scanning microscope (model Axiovert 100 M; Carl Zeiss MicroImaging, Inc.).

Wound healing

Wounding and wound closure measurements. Full thickness skin wounds were done in 2–3-mo-old male mice (n = 12 per genotype) in two independent experiments. Genotypes were blind to the researcher and observer. In brief, animals previously anesthetized with Avertin, were shaved, swabbed with 70% ethanol and two circular, full thickness excisional wounds (5-mm diam, separated by 10 mm) were created on their backs, by excising the skin and panniculus carnosus. The mice were housed individually. For macroscopic analysis, mice were monitored daily and wounds were photographed and measured at each time point (0, 3, 5, 7, 10, and 14 d) to analyze the healing process.

Preparation, analysis, and histology of wound tissues. For histology of wounds, six 3-mo-old male mice from each genotype were killed at each time point (1, 3, 5, 7, 10, and 14 d), and their wounds were harvested by complete excision including the 3 mm of the epithelial margins. Wounds were immediately fixed in 2% formaldehyde in PBS containing 0.02% NP-

40 at 4°C for 3 h. They were placed in 2% formaldehyde in PBS, left overnight in the cold, and paraffin embedded. 3–5-mm sections from the middle of the wounds were stained with hematoxylin-eosin and analyzed by light microscopy. The analysis of the wound tissue at day 7 was performed in groups of eight mice per genotype in three independent experiments showing similar results. For basal lamina immunohistochemistry of the wounds, we used the polyclonal antilaminin antibody from Biogenex as described by the manufacturers.

BrdU incorporation. To allow the analysis of the cell proliferation in the wounds, the nucleoside analogue BrdU (250 mg/kg of body weight) was injected i.p. 2 h before the animals were killed (eight animals per each genotype, day 7 after wounding). Samples were prepared as described in the previous paragraph. Incorporation of i.p.-injected BrdU into DNA of replicating cells was analyzed using anti-BrdU mAbs conjugated with alkaline phosphatase as described by the manufacturer (BrdU-labeling and detection kit II; Roche). The day 7 time point with BrdU labeling was also performed with six 11-mo-old male mice per genotype. Representative data are shown in the figures.

Statistical methods

Data analyses were performed with the use of the software package GraphPad PRISM, version 2.0. Data were summarized with the mean as a measure of central tendency and the standard error as a measure of dispersion. The differences in proportions between the wild-type and mutant mice were assessed by using the χ^2 and the Fisher Exact test. A p-value of 0.05 was chosen as the limit of statistical significance. Log-rank test statistical analysis was used to evaluate the survival curves.

Online supplemental material

The online supplemental material section contains the rationale used for the optimization of splice sites and RNAse protection analysis of liver samples from control and mutant mice (see Figs. S1 and S2, respectively). The experimental analysis of allele frequencies, offspring, and embryos is also described. Northern blot analysis and TUNEL and caspase-3 analysis of skin wounds are shown in Figs. S3 and S4, respectively. Online supplemental material is available at http://www.jcb.org/cgi/content/full/jcb.200212079/DC1.

We thank Dr. Pierre Chambon (Institut de Génétique et de Biologie, Strasbourg, France) for the CRE-transgenic mice; G. Faulkner for critical reading of the manuscript; and Giancarlo Lunazzi and Mauro Sturnega for animal care.

Submitted: 13 December 2002
Revised: 12 May 2003
Accepted: 16 May 2003

References

Boyle, D.L., Y. Shi, S. Gay, and G.S. Firestein. 2000. Regulation of CS1 fibronectin expression and function by IL-1 in endothelial cells. *Cell. Immunol.* 200:1–7.

Caputi, M., G. Casari, S. Guenzi, R. Tagliabue, A. Sidoli, C.A. Melo, and F.E. Baralle. 1994. A novel bipartite splicing enhancer modulates the differential processing of the human fibronectin EDA exon. *Nucleic Acids Res.* 22:1018–1022.

Caputi, M., F.E. Baralle, and C.A. Melo. 1995. Analysis of the linkage between fibronectin alternative spliced sites during ageing in rat tissues. *Biochim. Biophys. Acta.* 1263:53–59.

Chomczynski, P., and N. Sacchi. 1987. Single-step method of RNA isolation by acid guanidinium thiocyanate-phenol-chloroform extraction. *Anal. Biochem.* 162:156–159.

Clark, R.A., J.M. Lanigan, P. DellaPelle, E. Manseau, H.F. Dvorak, and R.B. Colvin. 1982. Fibronectin and fibrin provide a provisional matrix for epidermal cell migration during wound reepithelialization. *J. Invest. Dermatol.* 79: 264–269.

Clark, R.A., H.J. Winn, H.F. Dvorak, and R.B. Colvin. 1983. Fibronectin beneath reepithelializing epidermis in vivo: sources and significance. *J. Invest. Dermatol.* 80:26s–30s.

DeSimone, D.W., P.A. Norton, and R.O. Hynes. 1992. Identification and characterization of alternatively spliced fibronectin mRNAs expressed in early Xenopus embryos. *Dev. Biol.* 149:357–369.

Du, H., M. Heur, M. Duanmu, G.A. Grabowski, D.Y. Hui, D.P. Witte, and J. Mishra. 2001. Lysosomal acid lipase-deficient mice: depletion of white and brown fat, severe hepatosplenomegaly, and shortened life span. *J. Lipid Res.* 42:489–500.

Du, K., Y. Peng, L.E. Greenbaum, B.A. Haber, and R. Taub. 1997. HRS/SRp40-mediated inclusion of the fibronectin EIIIB exon, a possible cause of increased EIIIB expression in proliferating liver. *Mol. Cell. Biol.* 17:4096–4104.

ffrench-Constant, C. 1995. Alternative splicing of fibronectin—many different proteins but few different functions. *Exp. Cell Res.* 221:261–271.

ffrench-Constant, C., and R.O. Hynes. 1989. Alternative splicing of fibronectin is temporally and spatially regulated in the chicken embryo. *Development.* 106: 375–388.

ffrench-Constant, C., L. Van de Water, H.F. Dvorak, and R.O. Hynes. 1989. Reappearance of an embryonic pattern of fibronectin splicing during wound healing in the adult rat. *J. Cell Biol.* 109:903–914.

Fukuda, T., N. Yoshida, Y. Kataoka, R. Manabe, Y. Mizuno-Horikawa, M. Sato, K. Kuriyama, N. Yasui, and K. Sekiguchi. 2002. Mice lacking the EDB segment of fibronectin develop normally but exhibit reduced cell growth and fibronectin matrix assembly in vitro. *Cancer Res.* 62:5603–5610.

George, E.L., E.N. Georges-Labouesse, R.S. Patel-King, H. Rayburn, and R.O. Hynes. 1993. Defects in mesoderm, neural tube and vascular development in mouse embryos lacking fibronectin. *Development.* 119:1079–1091.

Georges-Labouesse, E.N., E.L. George, H. Rayburn, and R.O. Hynes. 1996. Mesodermal development in mouse embryos mutant for fibronectin. *Dev. Dyn.* 207:145–156.

Gimond, C., C. Baudoin, R. van der Neut, D. Kramer, J. Calafat, and A. Sonnenberg. 1998. Cre-loxP–mediated inactivation of the α6A integrin splice variant in vivo: evidence for a specific functional role of α6A in lymphocyte migration but not in heart development. *J. Cell Biol.* 143:253–266.

Goodrick, C.L. 1975. Life-span and the inheritance of longevity of inbred mice. *J. Gerontol.* 30:257–263.

Grinnell, F. 1984. Fibronectin and wound healing. *J. Cell. Biochem.* 26:107–116.

Guan, J.L., J.E. Trevithick, and R.O. Hynes. 1990. Retroviral expression of alternatively spliced forms of rat fibronectin. *J. Cell Biol.* 110:833–847.

Gutman, A., and A.R. Kornblihtt. 1987. Identification of a third region of cell-specific alternative splicing in human fibronectin mRNA. *Proc. Natl. Acad. Sci. USA.* 84:7179–7182.

Helgason, C.D., J.E. Damen, P. Rosten, R. Grewal, P. Sorensen, S.M. Chappel, A. Borowski, F. Jirik, G. Krystal, and R.K. Humphries. 1998. Targeted disruption of SHIP leads to hemopoietic perturbations, lung pathology, and a shortened life span. *Genes Dev.* 12:1610–1620.

Homanics, G.E., N.L. Harrison, J.J. Quinlan, M.D. Krasowski, C.E. Rick, A.L. de Blas, A.K. Mehta, F. Kist, R.M. Mihalek, J.J. Aul, and L.L. Firestone. 1999. Normal electrophysiological and behavioral responses to ethanol in mice lacking the long splice variant of the gamma2 subunit of the gamma-aminobutyrate type A receptor. *Neuropharmacology.* 38:253–265.

Hynes, R.O. 1990. Fibronectins. Springer-Verlag New York Inc., New York. 544 pp.

Jarnagin, W.R., D.C. Rockey, V.E. Koteliansky, S.S. Wang, and D.M. Bissell. 1994. Expression of variant fibronectins in wound healing: cellular source and biological activity of the EIIIA segment in rat hepatic fibrogenesis. *J. Cell Biol.* 127:2037–2048.

Kornblihtt, A.R., and A. Gutman. 1988. Molecular biology of the extracellular matrix proteins. *Biol. Rev. Camb. Philos. Soc.* 63:465–507.

Kornblihtt, A.R., K. Vibe-Pedersen, and F.E. Baralle. 1983. Isolation and characterization of cDNA clones for human and bovine fibronectins. *Proc. Natl. Acad. Sci. USA.* 80:3218–3222.

Kornblihtt, A.R., K. Vibe-Pedersen, and F.E. Baralle. 1984. Human fibronectin: molecular cloning evidence for two mRNA species differing by an internal segment coding for a structural domain. *EMBO J.* 3:221–226.

Kornblihtt, A.R., C.G. Pesce, C.R. Alonso, P. Cramer, A. Srebrow, S. Werbajh, and A.F. Muro. 1996. The fibronectin gene as a model for splicing and transcription studies. *FASEB J.* 10:248–257.

Kunstyr, I., and H.G. Leuenberger. 1975. Gerontological data of C57BL/6J mice. I. Sex differences in survival curves. *J. Gerontol.* 30:157–162.

Kwan, K.Y., and J.C. Wang. 2001. Mice lacking DNA topoisomerase IIIbeta develop to maturity but show a reduced mean lifespan. *Proc. Natl. Acad. Sci. USA.* 98:5717–5721.

Lavigueur, A., H. La Branche, A.R. Kornblihtt, and B. Chabot. 1993. A splicing enhancer in the human fibronectin alternate ED1 exon interacts with SR proteins and stimulates U2 snRNP binding. *Genes Dev.* 7:2405–2417.

Lewandoski, M. 2001. Conditional control of gene expression in the mouse. *Nat. Rev. Genet.* 2:743–755.

Liao, Y.F., P.J. Gotwals, V.E. Koteliansky, D. Sheppard, and L. Van De Water. 2002. The EIIIA segment of fibronectin is a ligand for integrins alpha 9beta 1 and alpha 4beta 1 providing a novel mechanism for regulating cell adhesion by alternative splicing. *J. Biol. Chem.* 277:14467–14474.

Lim, L.P., and P.A. Sharp. 1998. Alternative splicing of the fibronectin EIIIB exon depends on specific TGCATG repeats. *Mol. Cell. Biol.* 18:3900–3906.

Magnuson, V.L., M. Young, D.G. Schattenberg, M.A. Mancini, D.L. Chen, B. Steffensen, and R.J. Klebe. 1991. The alternative splicing of fibronectin pre-mRNA is altered during aging and in response to growth factors. *J. Biol. Chem.* 266:14654–14662.

Manabe, R., N. Oh-e, and K. Sekiguchi. 1999. Alternatively spliced EDA segment regulates fibronectin-dependent cell cycle progression and mitogenic signal transduction. *J. Biol. Chem.* 274:5919–5924.

Manabe, R., N. Ohe, T. Maeda, T. Fukuda, and K. Sekiguchi. 1997. Modulation of cell-adhesive activity of fibronectin by the alternatively spliced EDA segment. *J. Cell Biol.* 139:295–307.

Mardon, H.J., G. Sebastio, and F.E. Baralle. 1987. A role for exon sequences in alternative splicing of the human fibronectin gene. *Nucleic Acids Res.* 15: 7725–7733.

Muro, A.F., A. Iaconcig, and F.E. Baralle. 1998. Regulation of the fibronectin EDA exon alternative splicing. Cooperative role of the exonic enhancer element and the 5′ splicing site. *FEBS Lett.* 437:137–141.

Muro, A.F., M. Caputi, R. Pariyarath, F. Pagani, E. Buratti, and F.E. Baralle. 1999. Regulation of fibronectin EDA exon alternative splicing: possible role of RNA secondary structure for enhancer display. *Mol. Cell. Biol.* 19:2657–2671.

Okamura, Y., M. Watari, E.S. Jerud, D.W. Young, S.T. Ishizaka, J. Rose, J.C. Chow, and J.F. Strauss III. 2001. The extra domain A of fibronectin activates Toll-like receptor 4. *J. Biol. Chem.* 276:10229–10233.

Oyama, F., Y. Murata, N. Suganuma, T. Kimura, K. Titani, and K. Sekiguchi. 1989. Patterns of alternative splicing of fibronectin pre-mRNA in human adult and fetal tissues. *Biochemistry.* 28:1428–1434.

Pagani, F., L. Zagato, C. Vergani, G. Casari, A. Sidoli, and F.E. Baralle. 1991. Tissue-specific splicing pattern of fibronectin messenger RNA precursor during development and aging in rat. *J. Cell Biol.* 113:1223–1229.

Peters, D.M., L.M. Portz, J. Fullenwider, and D.F. Mosher. 1990. Coassembly of plasma and cellular fibronectins into fibrils in human fibroblast cultures. *J. Cell Biol.* 111:249–256.

Petersen, T.E., H.C. Thogersen, K. Skorstengaard, K. Vibe-Pedersen, P. Sahl, L. Sottrup-Jensen, and S. Magnusson. 1983. Partial primary structure of bovine plasma fibronectin: three types of internal homology. *Proc. Natl. Acad. Sci. USA.* 80:137–141.

Sakai, T., K.J. Johnson, M. Murozono, K. Sakai, M.A. Magnuson, T. Wieloch, T. Cronberg, A. Isshiki, H.P. Erickson, and R. Fassler. 2001. Plasma fibronectin supports neuronal survival and reduces brain injury following transient focal cerebral ischemia but is not essential for skin-wound healing and hemostasis. *Nat. Med.* 7:324–330.

Satoi, S., Y. Hiramatsu, H. Kitade, A.H. Kwon, K. Matsui, K. Miyashita, E. Sakashita, K. Sekiguchi, H. Takahashi, and Y. Kamiyama. 1999. Different responses to surgical stress between extra domain A+ and plasma fibronectins. *Clin. Exp. Pharmacol. Physiol.* 26:225–229.

Schwarzbauer, J.E., J.W. Tamkun, I.R. Lemischka, and R.O. Hynes. 1983. Three different fibronectin mRNAs arise by alternative splicing within the coding region. *Cell.* 35:421–431.

Schwarzbauer, J.E., R.S. Patel, D. Fonda, and R.O. Hynes. 1987. Multiple sites of alternative splicing of the rat fibronectin gene transcript. *EMBO J.* 6:2573–2580.

Schwarzbauer, J.E., C.S. Spencer, and C.L. Wilson. 1989. Selective secretion of alternatively spliced fibronectin variants. *J. Cell Biol.* 109:3445–3453.

Singh, S., R. Mishra, N.A. Arango, J.M. Deng, R.R. Behringer, and G.F. Saunders. 2002. Iris hypoplasia in mice that lack the alternatively spliced Pax6(5a) isoform. *Proc. Natl. Acad. Sci. USA.* 99:6812–6815.

Smith, G.S., R.L. Walford, and M.R. Mickey. 1973. Lifespan and incidence of cancer and other diseases in selected long-lived inbred mice and their F 1 hybrids. *J. Natl. Cancer Inst.* 50:1195–1213.

Sternlicht, M.D., and Z. Werb. 2001. How matrix metalloproteinases regulate cell behavior. *Annu. Rev. Cell Dev. Biol.* 17:463–516.

Tamkun, J.W., and R.O. Hynes. 1983. Plasma fibronectin is synthesized and secreted by hepatocytes. *J. Biol. Chem.* 258:4641–4647.

Usiello, A., J.H. Baik, F. Rouge-Pont, R. Picetti, A. Dierich, M. LeMeur, P.V. Piazza, and E. Borrelli. 2000. Distinct functions of the two isoforms of dopamine D2 receptors. *Nature.* 408:199–203.

Wang, A., D.S. Cohen, E. Palmer, and D. Sheppard. 1991. Polarized regulation of fibronectin secretion and alternative splicing by transforming growth factor. *J. Biol. Chem.* 266:15598–15601.

Wang, Y., R. Xu, T. Sasaoka, S. Tonegawa, M.P. Kung, and E.B. Sankoorikal. 2000. Dopamine D2 long receptor-deficient mice display alterations in striatum-dependent functions. *J. Neurosci.* 20:8305–8314.

Xia, P., and L.A. Culp. 1995. Adhesion activity in fibronectin's alternatively spliced domain EDa (EIIIA): complementarity to plasma fibronectin functions. *Exp. Cell Res.* 217:517–527.

Yoo, J.Y., D.L. Huso, D. Nathans, and S. Desiderio. 2002. Specific ablation of Stat3beta distorts the pattern of Stat3-responsive gene expression and impairs recovery from endotoxic shock. *Cell.* 108:331–344.

Zardi, L., B. Carnemolla, A. Siri, T.E. Petersen, G. Paolella, G. Sebastio, and F.E. Baralle. 1987. Transformed human cells produce a new fibronectin isoform by preferential alternative splicing of a previously unobserved exon. *EMBO J.* 6:2337–2342.